



**HAL**  
open science

# Rheological properties of artificial boluses of cereal foods enriched with legume proteins

F. Gibouin, R. van Der Sman, J. Benedito, G. Della Valle

## ► To cite this version:

F. Gibouin, R. van Der Sman, J. Benedito, G. Della Valle. Rheological properties of artificial boluses of cereal foods enriched with legume proteins. *Food Hydrocolloids*, 2022, 122, pp.107096. 10.1016/j.foodhyd.2021.107096 . hal-03351218

**HAL Id: hal-03351218**

**<https://hal.inrae.fr/hal-03351218>**

Submitted on 22 Aug 2023

**HAL** is a multi-disciplinary open access archive for the deposit and dissemination of scientific research documents, whether they are published or not. The documents may come from teaching and research institutions in France or abroad, or from public or private research centers.

L'archive ouverte pluridisciplinaire **HAL**, est destinée au dépôt et à la diffusion de documents scientifiques de niveau recherche, publiés ou non, émanant des établissements d'enseignement et de recherche français ou étrangers, des laboratoires publics ou privés.



Distributed under a Creative Commons Attribution - NonCommercial 4.0 International License

1 **Rheological properties of artificial boluses of cereal foods enriched with legume proteins**

2 F. Gibouin<sup>1</sup>, R. van der Sman<sup>2</sup>, J. Benedito<sup>3</sup>, G. Della Valle<sup>1\*</sup>

3 <sup>1</sup>INRAE UR-1268 Biopolymères Interactions et Assemblages, 44316 Nantes, France

4 <sup>2</sup>Agrotechnology and Food Sciences, Wageningen University and Research, 6708 WG Wageningen,  
5 The Netherlands

6 <sup>3</sup>Universitat Politècnica de Valencia, Departamento de Tecnología de Alimentos, 46071, Valencia,  
7 Spain

8 \* corresponding author: [guy.della-valle@inrae.fr](mailto:guy.della-valle@inrae.fr)

9 **Abstract**

10 The properties of artificial food bolus are studied by dynamic oscillatory and capillary  
11 rheometry as functions of bolus water content (WC), in the usual range of saliva hydration, for four  
12 cereal products: sponge cake, extruded flat bread and their counterpart enriched in legume proteins.  
13 All boluses followed the same rheological behaviour characterised by (1) solid -like in the linear  
14 viscoelastic domain and (2) Herschel-Bulkley model for large shear strain. Hence, four characteristic  
15 rheological properties are determined: modulus at viscoelastic plateau, characteristic stress at  
16 transition to flow, yield stress and consistency in the flow regime. The decrease of these properties  
17 with WC was fitted by an exponential decay function, from which was extracted a coefficient  $\alpha$   
18 ( $5 \leq \alpha \leq 30$ ), defined as a coefficient of interaction of the food with water. The values of  $\alpha$  are of  
19 the same order of magnitude as the plasticization coefficient of starch by water. They were larger for  
20 the extruded pea based (EFP,  $\alpha \geq 15$ ), and were lower for the sponge cake (SC,  $\alpha \leq 15$ ). The  
21 variations for the different rheological properties are discussed in terms of matter state, envisioning  
22 bolus as a suspension of soft swellable particles. The comparison of these values with those  
23 encountered for real boluses from similar foods suggests that these results contribute to define a  
24 coefficient of interaction of food with saliva.

25

26

27 **Keywords:** Herschel-Bulkley model; interaction coefficient; modulus; plant protein; viscosity

28

29

30 **Nomenclature**

31	$a$	shift factor used to derive the flow master curve
32	$D, D_p$	diameters of rheometer capillary die and piston, respectively
33	EF, EFP	extruded flat bread end extruded pea based snack, respectively
34	$G', G'', G^*$	storage, dissipative and complex modulus, respectively
35	$G'_0$	theoretical value of storage modulus for dry bolus
36	$K, K_c$	consistency and its corrected value in the Herschel-Bulkley model
37	$K_{c0}$	theoretical value of consistency for the dry bolus
38	$L/D$	length to diameter capillary die ratio
39	$n$	flow index in the Herschel-Bulkley model
40	SC, SCP	sponge cake, enriched in pulse protein, respectively
41	$T$	temperature
42	WC	Water content, expressed on a total wet basis
43	$\alpha_G, \alpha_{\tau_c}, \alpha_{\tau_y}, \alpha_K$	interaction coefficients of food with water based storage modulus, characteristic
44		stress, yield stress, consistency, respectively
45	$\gamma, \gamma_c$	strain and its value at intersection of $G'$ and $G''$ curves
46	$\dot{\gamma}_{app}, \dot{\gamma}_w$	apparent and real wall shear rate
47	$\dot{\epsilon}$	deformation rate
48	$\eta_{app}, \eta^*, \eta, \eta_E$	apparent, complex, shear and elongational viscosity, respectively
49	$\omega$	pulsation (oscillatory rheometry tests)
50	$\tau_w, \tau_c, \tau_s, \tau_{sc}$	wall shear, characteristic, yield (Hersche-Bulkley), corrected stress
51	$\tau_{c0}, \tau_{s0}$	dry bolus theoretical values of characteristic and yield stress, respectively

52

53

## 54 1. Introduction

55 Food Oral Processing (FOP) is a key step for food digestion. Its first aim is to form a food  
56 bolus that can be swallowed safely (Chen, 2009 ; Stokes, Boehm & Baier, 2013). It is also the first  
57 interaction of our body with food in the digestive system. During oral processing, food is reduced in  
58 size and lubricated to form a bolus in preparation for swallowing and digestion. Simultaneously,  
59 volatile chemicals from the food move to olfactory and taste receptors, food particles interact with  
60 oral surfaces, and the net result is an evaluation of taste, aroma, and texture. The rheological  
61 properties of the bolus are a link between food texture, its breakdown and its capacity to be  
62 swallowed, and they are modified by the saliva uptake. Consequently, the knowledge of bolus  
63 rheological properties is important to understand the dynamic changes in food structure that take  
64 place during FOP (Morell, Hernando & Fiszman, 2014). Consequently, there is a need to develop  
65 methods for assessing food breakdown during chewing and interaction with saliva (Boehm, Warren,  
66 Baier, Gidley & Stokes, 2019).

67 The food bolus experiences a large range of shear rate and also extensional flow during oral  
68 processing. From apparent viscosity ( $\eta_{app}$ ) measurements, a model was built to represent the bolus  
69 breakdown of cereal foods, such as sponge cake and brioche, during chewing (Assad-Bustillos,  
70 Tournier, Septier, Della Valle & Feron, 2019a). This model allowed to derive a coefficient relating  
71 bolus viscosity to its water content, which was defined as a coefficient of interaction «  $\alpha$  » between  
72 saliva and food (Assad-Bustillos et al., 2020). The variations of  $\alpha$  underlined the influence of protein  
73 enrichment on the oral processing of these cereal foods. It also showed that the study of FOP is an  
74 essential step in food design, in the case of enrichment of foods by legume proteins. Moreover, a  
75 correlation between  $\eta_{app}$  with oral comfort for low fat cereal foods has been established, which just  
76 confirmed how important are the bolus shear and extensional viscosities for the ease of swallowing  
77 (Marconati et al., 2019).

78 Saliva contains water at 99%, plus other components, such as mucin, and its properties have  
79 a large variability depending on individual and stimulation conditions (Haward, Odell, Berry & Hall,  
80 2011; Mosca & Chen, 2017). So the increase of bolus water content (WC), due to saliva flow during  
81 chewing, is a common important feature in FOP. This is especially true for cereal products which  
82 contain a large amount of amorphous starch, knowing the role of water as a plasticizer for  
83 hydrophilic food components, such as amorphous starch. So, there is an interest to study the WC  
84 dependence of bolus rheological properties of cereal food boluses and, by extent, to any food that  
85 contains hydrophilic compounds.

86 Surprisingly, there are quite few studies dealing with the rheological properties of food bolus.  
87 This can be due (1) to the difficulty of performing rheological measurements on real boluses, and (2)

88 to the uncertainty about the relevant rheological property for food oral processing. To overcome the  
89 former difficulty, artificial boluses can be considered, provided that they are representative of real  
90 ones. By doing so, it is possible to address the latter difficulty by performing different rheological  
91 tests under a wide range of strain and strain rate conditions.

92           Given this context, the aim of this work is to determine the rheological properties of artificial  
93 boluses of cereal foods in order to derive coefficients that help to quantify the interactions of foods  
94 with saliva. For this purpose, artificial boluses are prepared under conditions as close as possible to  
95 those encountered in FOP, to avoid physiological interindividual variability and to focus on bolus  
96 rheology and the influence of water content. Bolus viscoelastic properties are investigated in the  
97 linear and non-linear viscoelastic domains, using oscillatory shear rheometry, and flow properties are  
98 measured by capillary rheometry. In addition to insights on food bolus structure, the variations of the  
99 rheological properties with WC are determined for two types of cereal foods: a soft food with  
100 intermediate moisture and a brittle dry one, as well as their corresponding version enriched in plant  
101 protein.

102  
103

## 104 **2. Material and methods**

### 105 ***2.1. Cereal foods and bolus preparation***

106           Four cereal food products were studied: two soft foods (sponge cake, SC) and two brittle  
107 ones (extruded, E). One SC had a standard formulation (SC) and the other one was enriched with pea  
108 proteins and held the claim “high in protein” (SCP). Both were provided by CERELAB® (Aiseray,  
109 France). One extruded food is a commercial flat bread (EF, Les craquantes EPI d’OR™) and the other  
110 one is made by extrusion of pea flour (EFP), as described in detail by Kristiawan et al. (2018). Their  
111 composition, moisture content and density are reported in Table 1. Besides various differences,  
112 especially starch content, the difference of water content makes the food soft (SC) or brittle (E).

113           In order to prepare artificial boluses, foods were fragmented and impregnated with water,  
114 the main component (99%) of human saliva. This study focuses on the role of water, because the  
115 addition of mucin and salts has been precedingly shown not to modify the rheological properties of  
116 sponge cake boluses (Gibouin, Della Valle & van der Sman, 2019 a,b). In addition, the role of  $\alpha$ -  
117 amylase on rheological properties is discarded, in a first approach. The role of real saliva, and  
118 especially of  $\alpha$ -amylase will be discussed when comparing our results with those obtained for real  
119 boluses, in section 3.3. Water was added at different levels, in order to obtain a bolus, homogeneous  
120 at bare eye, and to cover the range of water content of food bolus during chewing, in agreement  
121 with values found in literature, up to 60% for sponge cake and 80% extruded foods, in total wet  
122 content (Assad-Bustillos et al., 2019a; Loret et al., 2011).

123 Before water addition, sponge cakes and extruded foods were fragmented with a commercial  
124 blender(MagiMix, France) or manually using a mortar, respectively, until a particle mean size of 1mm  
125 is reached, as measured with a vibrating sieves (Reitsch, F95610 Eragny). This size value is chosen  
126 close enough to the particle size in real boluses at the first step of chewing. It has also been checked  
127 that the particle size distribution is in agreement with the distribution in real boluses (Assad-Bustillos  
128 et al., 2019b), and that in the range [1, 10mm], the particle size did not affect significantly the  
129 rheological properties (Gibouin et al., 2019 a,b).

### 130 **2.2. Viscoelastic properties and oscillatory shear measurements**

131 Viscoelastic properties of bolus were determined with a controlled strain rheometer (ARES,  
132 TA Instruments), provided with a plate-plate circular geometry: diameter = 4.0cm and gap = 2.5mm.  
133 The temperature is controlled with a Peltier device and set to 23°C. The bolus sample is placed on the  
134 lower plate and is gently squeezed to ensure surface contact. The variations of storage ( $G'$ ) and loss  
135 ( $G''$ ) moduli, with strain were determined at three different frequencies:  $\omega = 10\text{rad/s}$ ,  $\omega = 1\text{rad/s}$   
136 and  $\omega = 0.1\text{rad/s}$ . The imposed strains ranged from 0.01% to 400% according to a logarithmic  
137 distribution and with 10 points per decade. Each measurement is duplicated and the sample is  
138 removed and replaced before each test. Moduli and complex viscosity  $\eta^*$  were determined in the  
139 linear viscoelastic regime (imposed strain  $\gamma = 0.5\%$ ) by applying a frequency sweep from 0.1rad/s to  
140 100rad/s. The frequency distributions are also logarithmic with 10 points per decade and the  
141 measurements are duplicated. All these measurements were achieved on bolus with various water  
142 contents WC from 0.3 to 0.57 kg water / kg bolus on total wb (SC, SCP) and 0.68 to 0.8 kg water / kg  
143 bolus on total wb (EF, EFP), in total wet basis.

### 144 **2.3. Flow properties and capillary rheometry measurements**

145 Flow properties are determined with a capillary rheometer with pre-shearing, Rheoplast, that  
146 has been applied and described in detail by Della Valle, Vergnes & Lourdin (2007) and Nunez, Della  
147 Valle & Sandoval (2010), who determined the viscous properties of starchy materials and cereal  
148 foods, respectively, under extrusion conditions. In the following, we will only describe its main  
149 working steps. In the case of food bolus, we did not use the pre-shearing function, because the  
150 fragmentation has already been performed when preparing bolus with the blender.

151 All the tests are made at room temperature ( $T = 23^\circ\text{C}$ ). The measuring chamber before the  
152 capillary die is fed with the bolus by the vertical motion of an annular piston at a constant speed of  
153 1mm/s. Then, the injection piston (diameter  $D_p = 16\text{mm}$ ) is moved vertically at a constant speed of  
154 0.5mm/s to fill the capillary die. Three capillary dies (diameter  $D = 1\text{mm}$ , entry angle =  $90^\circ$ ) are used  
155 with different die ratios  $L/D$  (32, 16 and 8). After a 15 s relaxation time, pressure is measured for  
156 different decreasing speeds of the injection piston, each speed step for a time interval of about 15s,

157 ranging from 2 mm/s to 0.002mm/s, which leads to apparent shear rate values  $3000 \geq \dot{\gamma}_{app} \geq 3 \text{ s}^{-1}$ .  
158 At the end of this sequence (about 2 mn), pressure measurement is repeated at the two largest  
159 speed values, in order to check sample stability, and a pressure profile  $P(\dot{\gamma}_{app})$  is obtained.

160 This procedure has been applied to every sample for the same range of water content values  
161 as for oscillatory shear measurements (2.2). 15 to 20g of bolus are needed to obtain a single pressure  
162 profile. Data treatment is performed according to usual procedure for capillary rheometry as  
163 described in detail by Della Valle et al. (2007) and Nunez et al. (2010). The wall stress  $\tau_w$  is derived  
164 from pressure measurements, using Poiseuille law, after application of Bagley's corrections. The flow  
165 index  $n$  is determined and the real value of the shear rate  $\dot{\gamma}_w$  is calculated after Rabinowitsch  
166 analysis. Finally, the shear viscosity  $\eta$  is defined as the ratio  $\tau_w/\dot{\gamma}_w$ . Using entrance effects from  
167 Bagley correction, the elongational viscosity  $\eta_E$  and the deformation rate  $\dot{\epsilon}$  may also be derived,  
168 according to the Cogswell's method developed for melts polymers (Cogswell, 1972).

169 Flow curves ( $\tau_w$  or  $\eta(\dot{\gamma}_w)$ ) obtained for different moisture contents were fitted according to  
170 appropriate rheological model and then shifted (translated) into a master curve to determine the  
171 model parameters. This procedure, based on the time-temperature superposition principle, for the  
172 rheological properties of polymers, has been already adapted by Della Valle et al. (2007) to the time-  
173 plasticizer content superposition, in the case of plasticized starches. In this study, the shifting factors  
174 were derived using Python (Python Software Foundation) according to the procedure developed by  
175 Saboo *et al.* (2018).

## 176 **2.4 Imaging**

177 Fragmented boluses of sponge cakes and extruded foods were prepared in the same way as  
178 for rheological measurements and water was added to obtain the necessary dilution before inserting  
179 between glass blades, and observed on a binocular stereomicroscope Leica with retro-lighting ( $\times 35$  ;  
180 Leica Microsystems, Conrad Electronics, France ). No specific staining was used.

181

182

## 183 **3. Results and discussion**

### 184 **3.1. Viscoelastic properties**

185 Within the linear domain ( $\gamma < 1\%$ ), harmonic measurements performed at small strain  
186 amplitude, led to similar bolus mechanical spectra ( $G'(\omega)$ ,  $G''(\omega)$ ) whatever the food considered and  
187 its water content (Fig.1) :  $G'$  and  $G''$  were slightly increasing functions of pulsation (or frequency) and  
188 all bolus exhibited a storage modulus larger than the dissipative one ( $G' > G''$ ) in the range of  
189 frequency tested, and  $\tan \delta$  remained nearly constant ( $\approx 0.2$ ). Clearly boluses behave more like solid  
190 than fluids. Such spectra are usually typical of a viscoelastic network, with the frequency window of

191 the test framing a part of the viscoelastic plateau. However, in the case of these artificial bolus, no  
192 structural interpretation can be given for the entities involved in such a network, at this stage. In  
193 many cases,  $G''(\omega)$  curves exhibited a shallow minimum within the frequency interval ( $0.1 < \omega < 1$   
194  $\text{rd/s}$ ). The frequency and the  $G'$  value corresponding to this  $G''$  minimum can be taken conventionally  
195 as representative of the characteristics (frequency and modulus) of the viscoelastic plateau  
196 (Ferry,1980). However, the frequency of the minimum depended on the bolus, and in some cases, it  
197 was not really observed. Therefore, for all our samples, we took the  $G'$  value at  $1 \text{ rad/s}$  as an  
198 empirical measure of the viscoelastic plateau modulus. Fig.1 also showed that, for all food boluses, a  
199 regular decrease of both moduli was observed as water content increased, which, as expected,  
200 indicated that water acts as a lubricant. It also suggested that, for SC bolus, the enrichment in protein  
201 slightly increased the values of moduli, and reduced its sensitivity to water content. Conversely, pea  
202 based extruded snacks (EFP) led to boli with much larger moduli, about 10 times, than extruded flat  
203 bread (EF), but displayed similar water sensitivity.

204 The values of storage modulus at viscoelastic plateau  $G'(\omega \leq 1 \text{ rd/s})$  were negatively  
205 correlated to the water content (Fig.2). These variations can be described by the equation :

$$206 \quad G' = G'_0 * \exp [ - \alpha_G * WC ] \quad (1)$$

207  $G'_0$  represents the theoretical value of storage modulus for dry bolus ; parameter  $\alpha_G$ . reflects  
208 the interaction of the food with water and can be envisioned as a water plasticization coefficient. The  
209 values of these parameters are reported in Table 2. Similar results could have been obtained by  
210 shifting and superimposing  $G'$  (and  $G''$ ) curves for a given moisture content as performed by van der  
211 Sman and Mauer (2019), in the case of starch/sugar/polyol mixtures, and by Costanzo et al. (2019)  
212 for gluten / water / ethanol blends. Besides extending the time-temperature superimposition  
213 principle to time-solvent in the case of biopolymers, these works underlined the importance of  
214 intermolecular interactions, mainly H bonds. Such interactions could be captured by the ratio of  
215 sample temperature to glass transition temperature of the biopolymer, which is a function of its  
216 solvent content. Regarding food boluses, our results suggest that the protein enriched sponge cake  
217 (SCP) interacts the least with water, likely because of the hydrophobic nature of added pea isolates,  
218 whereas globulins interactions with glutenins might also be inferred for the decrease of water  
219 sensitivity (Lambrecht, Deleu, Rombouts & Delcour, 2018). Conversely, extruded pea flour (EFP)  
220 shows larger interaction with water than flat bread (EF), likely because hemicellulosic compounds,  
221 contained in pea flour, have a strong water retention capacity that largely balances the hydrophobic  
222 influence of pea isolates observed for SCP (Kristiawan et al., 2018).

223 For all moisture contents and foods, the variations of  $G'$  and  $G''$  moduli with the applied  
224 strain  $\gamma$  exhibited the same patterns (Fig. 3). From this graph, three main zones may be delineated:



225 first the linear viscoelastic regime ( $\gamma \leq 1\%$ ), where moduli are constant, with  $G' > G''$  like for a gel,  
 226 then, a transient regime, where storage modulus decreases and crosses  $G''$  curve, which can be  
 227 considered as plastic region, and, finally, a non-linear regime where both moduli decrease, with  $G'' >$   
 228  $G'$ , indicating that bolus starts to flow. This behaviour is typical of the loss of structure and of the  
 229 flow of the material under increased strain. Since it holds for all bolus samples, we can define the  
 230 stress  $\tau_c$ , at the crossing of  $G'$  and  $G''$  as a characteristic parameter of this behaviour:

$$231 \quad \tau_c = \gamma_c * G^* \quad (2)$$

232  $G^*$  being the value of the complex modulus and  $\gamma_c$  the strain value at intersection of  $G'$  and  
 233  $G''$  curves ( $G'=G''$ ). Another characteristic stress maybe defined, by the value obtained at the end of  
 234 the linear viscoelastic domain, defined by the crossing of the horizontal tangent of  $G'$  in the linear  
 235 domain with the tangent to  $G'$  curve during plastic flow (see Fig.3). It is found that these values are  
 236 highly correlated to the values of  $\tau_c$  ( $r^2 > 0.9$ , see Appendix 1), so, in the following,  $\tau_c$  is considered to  
 237 characterise the transition of bolus to flow. The values of  $\tau_c$  are negatively correlated to the water  
 238 content (Fig.4). These variations can be described by the equation :

$$239 \quad \tau_c = \tau_{c0} * \exp [ - \alpha_{\tau_c} * WC ] \quad (3)$$

240  $\tau_{c0}$  is the theoretical value of characteristic stress for the dry bolus; parameter  $\alpha_{\tau_c}$  reflects the  
 241 interaction of the food with water, like a water plasticization coefficient. The values of these  
 242 parameters are reported in Table 2. At first glance, they confirm the trends observed in the linear  
 243 viscoelastic domain, when considering  $\alpha_G$  values : protein enriched sponge cake (SCP) interacts the  
 244 least with water, again due to the hydrophobicity of pea isolates, whereas extruded pea flour (EFP)  
 245 shows larger interaction with water than flat bread (EF), which, again, may be attributed to the  
 246 presence of hemicellulosic compounds in pea flour. However, for extruded products, the values of  
 247  $\alpha_{\tau_c}$  are larger than those of sponge cakes, and the variations of characteristic stress obtained for EF  
 248 and EFP are close to each other (Fig.4). This result indicates that the stress needed to make the bolus  
 249 flow is more influenced by water for extruded cereal foods, than for sponge cakes, whether they are  
 250 enriched in plant proteins or not. Moreover, the huge value of initial stress  $\tau_{c0}$ , found for extruded  
 251 products (Table 2,  $\tau_{c0} > 100$  MPa), confirms that, overall, large amounts of water ( $WC \geq 60\%$ ) are  
 252 needed to elaborate a flowable bolus from these foods that contain a large amount of hydrophilic  
 253 compounds like amorphous starch.

254

### 255 **3.2 Flow properties**

256 From the pressure profiles  $P(\dot{\gamma}_{app})$  obtained for different capillary geometries (L/D ratio),  
 257 and using Poiseuille relation, flow curves can be derived, representing the variations of the wall shear

258 stress  $\tau_w$  as a function of apparent shear rate or  $\tau_w (\dot{\gamma}_{app})$  for food boluses at different amount of  
 259 water WC (Fig.5). As expected, the larger WC, the lower the apparent viscosity, defined by the ratio  
 260  $\tau_w/\dot{\gamma}_{app}$  : flow curves show that viscosity decreases by a factor of 10 when WC is increased by 0.10  
 261 for SC foods, whereas the decrease is lower for extruded foods. Some curves display a dispersion of  
 262 experimental points, especially at larger moisture content. Indeed, in these conditions, flow becomes  
 263 less steady and measurement accuracy lower, given the low level of pressure reached in the  
 264 capillary, and also possible slip-stick phenomena. However, all curves show a similar increasing trend,  
 265 and some of them suggest the existence of a yield stress at lower shear rate (like for SC at WC= 0.28  
 266 and 0.36, for instance). Therefore, after having converted apparent shear rate values  $\dot{\gamma}_{app}$  into wall  
 267 shear rate  $\dot{\gamma}_w$ , using Rabinowitsch correction, all curves are fitted using the Herschel-Bulkley model,:

$$\tau_w = \tau_s + K * \dot{\gamma}_w^n \quad (4)$$

269 where  $\tau_s$  is the yield stress,  $K$  the consistency (Pa.s<sup>n</sup>), and  $n$  the flow index.

270 Although fitting is acceptable ( $r^2 > 0.75$ ), considering the dispersion mentioned before, it is thought  
 271 that determining coefficients  $\tau_s$ ,  $K$  and  $n$  for each WC value could increase the uncertainty. Moreover,  
 272 the flow index does not change significantly for each product, whatever the value of WC. Therefore,  
 273 for each product, a master curve is determined by adapting the time-temperature principle, to  
 274 superpose flow curves, obtained from bolus at different water content. Hence, each flow curve is  
 275 shifted to a reference curve, at a given WC value, by plotting the reduced shear stress ( $\tau_w / a$ ) as  
 276 function of reduced shear rate ( $\dot{\gamma}_w * a$ ),  $a$  being the shift factor. This procedure is illustrated in  
 277 Appendix 2. The Herschel-Bulkley coefficients of the reference curve are recalled in Table 3, for each  
 278 product. The values of the shift factor  $a$  vary between 0.016 and 27.8 and they are directly correlated  
 279 to the water content, all food products being considered together (Fig.6a). In a first approach, this  
 280 correlation suggests that the influence of water on the viscous behavior of the bolus in shear flow is  
 281 similar for the four different cereal foods. Secondly, by applying (eq.4) to  $(\tau_w/a) [a*\dot{\gamma}_w]$ , this  
 282 correlation can be used to calculate, for any WC value, the corrected values for the coefficients of the  
 283 Herschel Bulkley model by :

$$\tau_{sc} = \tau_s / a(WC) \quad \text{and} \quad K_c = K / [a(WC)]^{n+1} \quad (5)$$

284 The numerical values of  $\tau_{sc}$ ,  $K_c$  and  $n$ , for all values of WC and products tested, are reported  
 285 in Appendix 3. Note that the value of flow index  $n$  did not vary with WC. Furthermore, using  
 286 correlation from Fig.6a and eq. (5), flow curves for the boluses of the four products can be derived  
 287 for any WC value. For instance, for WC=0.6, taken as a typical value in the interval [0.28, 0,8], flow  
 288 curves representing the shear viscosity  $\eta$  as a function of shifted shear rate ( $\dot{\gamma}_w * a$ ) can be drawn  
 289 (Fig.6b). These curves show that for low shear rate values, the viscosity of the bolus is very close to  
 290 each other, whereas for larger values ( $\dot{\gamma}_w * a > 10s^{-1}$ ), the two extruded products (EF and EFP) lead to  
 291

292 much larger viscosity than sponge cakes, whether they are enriched in plant protein or not. The  
293 increase of slope, observed at lower shear rate values, underlines the presence of the yield stress,  
294 and it is enhanced for SC and EFP. In line with the preceding results obtained for the viscoelastic  
295 properties, the variations of the Herschel-Bulkley coefficients  $\tau_{sc}$  and  $K_c$  with WC can be represented  
296 (Fig.7) and fitted by the following relations :

$$297 \quad \tau_{sc} = \tau_{s0} \cdot \exp [ -\alpha_{\tau} * WC ] \quad \text{and} \quad K_c = K_{c0} \cdot \exp [ -\alpha_K * WC ] \quad (6)$$

298 from which the values of  $\tau_{s0}$ ,  $\alpha_{\tau}$ ,  $K_{c0}$  and  $\alpha_K$  are extracted and reported in Table 2. In  
299 addition, variations of consistency with water are very close to each other for the four products (Fig.  
300 7b), and a common trend can be found for  $K_c$  variations, giving a mean value for  $\alpha_K = 10.25$  ( $r^2 = 0.9$ ).  
301 Regarding  $\alpha_{\tau}$  and  $\alpha_K$  variations, the trends obtained here are different from those observed for the  
302 viscoelastic properties since standard products (SC and EF) display the lower  $\alpha_{\tau}$  and  $\alpha_K$  values.  
303 Moreover,  $\alpha_{\tau}$  and  $\alpha_K$  values are correlated. These results show that, during the flow, the products  
304 enriched with plant proteins interact more with water than their standard counterpart. In other  
305 words, the presence of proteins increase the bolus flow sensitivity to water, which suggests that flow  
306 could contribute to bolus destructuring by disrupting food particles or releasing protein aggregates.

307 The same procedure can be applied to determine the apparent elongational viscosity of  
308 boluses, by taking into account entrance pressure effects from capillary rheometry tests. Then, using  
309 the same time-water superposition principle, master curves can be determined, for instance at WC  
310 =0.6 (see Appendix 4). Indeed, very little differences can be observed between the four foods.

311

### 312 **3.3 Bolus structure and rheological properties relationships**

313 First, the values found for coefficients  $\alpha$  were in the same numerical interval [5, 31],  
314 regardless the rheological property. These values are in the same interval as the values of coefficients  
315 of starch plasticization by water, found for starchy materials and cereal foods under extrusion  
316 conditions (Della Valle et al., 2007; Nunez et al., 2010). Clearly, this result suggests that starch /water  
317 interactions have a significant role in the rheological behavior of the bolus and its breakdown during  
318 FOP. However, these values stand for starch melts as encountered during extrusion, i.e. at high  
319 temperature and shear, where starch granules are broken and polymers released. Food boluses can  
320 hardly be compared to starch melts. By the way, Cox-Merz rule does not apply, unlike polymer  
321 melts, since complex viscosity always took values larger than those of steady shear viscosity (as  
322 illustrated in Appendix 5), which reflects that the structure of bolus changed during steady flow.

323 Moreover, boluses are made of particles, of typical size 1mm, which are not expected to  
324 fragment during flow, but rather to deform, as shown by the micrographs of diluted boluses (Fig.8).  
325 Sponge cake (SC) bolus presents a rather uniform appearance of a cohesive mass of blurred

326 aggregated particles, whereas enriched protein sponge cake (SCP) is more heterogenous, with darker  
327 parts and bigger entities ( $> 1$  mm), separated by water. Extruded flat bread bolus (EF) also presents a  
328 cohesive morphology, whereas extruded pea flour bolus (EFP) presents a clear picture of  
329 agglomerated and elongated particles (length  $> 1$ mm, width  $< 1$ mm). These images suggest that the  
330 foods are not destructured in the same way after fragmentation and hydration. So it is not surprising  
331 that their characteristic rheological properties are not fully correlated.

332 In spite of these visual differences, they may be all envisioned as concentrated suspensions of  
333 deformable particles (Fig.9). At lower strain the suspension is jammed, because of particles swelling  
334 due to water absorption (Fig.9b), which gives the bolus a solid-like behavior, in the viscoelastic  
335 domain. At larger strain, hence larger stress ( $\tau > \tau_c$  or  $\tau_s$ ), the suspension may still be partially  
336 jammed, because, in the case of standard foods, hydrophilic particles still swell (Fig.9c). Conversely,  
337 the particles of protein enriched foods, being less hydrophilic, swell less, water acts as a lubricant  
338 which favors bolus flow (Fig. 9d). This interpretation would explain why the values of coefficient  $\alpha$   
339 referring to flow properties (yield stress  $\tau_s$  and consistency  $K$ ) are larger for the protein enriched  
340 foods than for their standard counterpart. More experiments, for instance using measurements of  
341 water absorption or swelling index on such products, and even comparison with settling ratio  
342 (Boehm et al. 2019) could contribute to test this hypothesis. Whether this transition occurs at the  
343 value of characteristic stress  $\tau_c$  or yield stress  $\tau_s$  is still to be determined precisely, although both  
344 properties are correlated (Fig.10). The question is significant since both properties might be relied on  
345 for the control of swallowing.

346 Clearly, before extending these rheological measurements to assess the interactions of saliva  
347 with food, it is necessary to test the influence of other saliva components on bolus rheological  
348 properties. Recently, these properties were measured on bolus made by mixing same foods (sponge  
349 cake) with artificial saliva, containing salt and mucin, and no significant difference was detected  
350 when compared with bolus made with water (Gibouin et al., 2019b). The influence of the addition of  
351  $\alpha$ -amylase, another component of saliva, on bolus rheological properties is still questionable. There is  
352 a general agreement that salivary  $\alpha$ -amylase plays an important part in destructuring cereal foods,  
353 like bread, during the gastric phase (Bonhorst & Singh, 2013; Pentikäinen et al., 2014; Freitas,  
354 Feunteun, Panouille & Souchon, 2018). But the short residence time of the food in the mouth may  
355 explain the little influence of  $\alpha$ -amylase on bread destructuring during FOP, assessed by viscosity  
356 measurements (Le Bleis, Chaunier, Montigaud & Della Valle, 2016).

357 Regarding FOP, another point that confirms the relevance of our measurements comes from  
358 some results obtained when characterizing real boluses. Results obtained by Loret et al. (2011)  
359 measuring yield stress on cereal flakes boluses collected before swallowing for 11 subjects, hence for

360 different saliva contents, lead to a value of  $\alpha$  of about 8, i.e. in the interval found in this study. For  
361 sponge cake boluses, the values of coefficient  $\alpha$  found for apparent viscosity were also in the same  
362 interval (17 and 11 for standard and protein enriched sponge cake, respectively) (Assad-Bustillos et  
363 al., 2020). Furthermore, they ordered in the same way as the values of  $\alpha_{\tau_c}$  found in the present  
364 study (9.3 and 4.8, see Table 2). This result suggests that the coefficient  $\alpha_{\tau_c}$  contributes to assess  
365 food-saliva interaction and that characteristic stress  $\tau_c$  is the property that matters to define bolus  
366 destructuring. Although more work is necessary to ascertain this trend, it is possible, and rather  
367 simple, to extend these rheological methods to other foods. In turn, this would help to design and  
368 test foods that would have a specific behavior during chewing.

369

370

#### 371 **4. Conclusion**

372 Our results show that the rheological properties of artificial food cereal boluses can be  
373 determined in a wide range of strain and strain rates, using different methods, in the range of water  
374 content encountered during FOP. For the four foods tested, hydrated boluses exhibited same  
375 behavior. First, at low strain, in the linear viscoelastic domain, bolus had a gel like behavior  
376 characterized by the viscoelastic modulus  $G^*$ . Then, destructuring occurs at larger strain ( $\gamma \geq 0.1$ ),  
377 where a characteristic stress  $\tau_c$  can be delineated from the intersection between curves of storage  
378 and dissipative moduli. During steady flow, bolus behavior was found to follow Herschel-Bulkley  
379 model from which yield stress  $\tau_s$  and consistency  $K$  were derived; master curves could be determined  
380 to compare the viscous behavior of the four products. At larger shear rate ( $\dot{\gamma}_w \geq 10 \text{ s}^{-1}$ ), viscosity was  
381 found larger for extruded foods without any effect of protein content. The variations of these four  
382 rheological properties ( $G^*$ ,  $\tau_c$ ,  $\tau_s$  and  $K$ ) with water followed an exponential decay, from which it was  
383 possible to derive coefficients of interaction with water, for each property and product. Their  
384 changes with product composition and structure were interpreted by envisioning the bolus as a  
385 suspension of soft particles. The comparison of their values with those obtained for real boluses, and  
386 their variations with protein content, suggest that rheological measurements are helpful to  
387 characterize the interaction of food with saliva. Finally, given the interest to study the water  
388 dependence of rheological properties of cereal food boluses, the same approach could apply to  
389 other food products too.

390

391

#### 392 **Acknowledgements**

393 This work was carried out with the financial support of the regional programme "Food for Tomorrow  
394 / Cap Aliment", which is supported by the French Region Pays de la Loire and the European Regional  
395 Development Fund (FEDER). Florence' stay at UPV received the support of COST Action (CA15118 -  
396 Mathematical and Computer Science Methods for Food Science and Industry).

397

398

399

400 **References**

- 401 Assad-Bustillos, M., Tournier, C., Septier, C., Della Valle, G., Feron, G. (2019a). Relationships of oral  
402 comfort perception and bolus properties in the elderly with salivary flow rate and oral health  
403 status for two soft cereal foods. *Food Research International*, 118, 13–21.
- 404 Assad-Bustillos, M., Tournier, C., Feron, G., Guessasma, S., Reguerre, A. L., Della Valle, G. (2019b).  
405 Fragmentation of two soft cereal products during oral processing in the elderly: Impact of  
406 product properties and oral health status. *Food Hydrocolloids*, 91, 153–165.
- 407 Assad-Bustillos, M., Tournier, C., Palier, J., Septier, C., Feron, G., Della Valle, G. (2020). Oral  
408 processing and comfort perception of soft cereal foods fortified with pulse proteins in the  
409 elderly with different oral health status. *Food & Function*, 11, 4535–4547.
- 410 Boehm, M.W., Warren, F.J., Baier, S.K., Gidley, M.J., Stokes, J.R. (2019). A method for developing  
411 structure-rheology relationships in comminuted plant-based food and non-ideal soft particle  
412 suspensions. *Food Hydrocolloids*, 96, 475–480.
- 413 Bonhorst, G.M., & Singh, P. (2013). Kinetics of *in Vitro* Bread Bolus Digestion with Varying Oral  
414 and Gastric Digestion Parameters. *Food Biophysics* 8, 50–59
- 415 Chen, J. (2009). Food oral processing. A review. *Food Hydrocolloids* 23, 1-25.
- 416 Cogswell, F. N. (1972). Converging flow of polymer melts in extrusion dies. *Polymer Engineering &*  
417 *Science*, 12, 64-73.
- 418 Costanzo S., Banc A., Louhichi A., Chauveau E., Wu BH., Morel MH., Ramos, L. (2020). Tailoring the  
419 Viscoelasticity of Polymer Gels of Gluten Proteins through Solvent Quality. *Macromolecules*  
420 53, 9470-9479.
- 421 Della Valle, G., Vergnes, V., and Lourdin, D. (2007). Viscous properties of thermoplastic starches from  
422 different botanical origin. *International Polymer Processing*, 22, 471-479. Ferry, J.D. (1980).  
423 Viscoelastic Properties of Polymers. Wiley, New York.
- 424 Freitas, D., Feunteun, S.L., Panouillé M., Souchon I. (2018). The important role of salivary  $\alpha$ -amylase  
425 in the gastric digestion of wheat bread starch. *Food & Function* 9, 200–208.
- 426 Gibouin, F., Della Valle, G. & van der Sman, R. (2019a). Mesures de viscosités de bols alimentaires  
427 artificiels. *Rhéologie* 36, 15-20.
- 428 Gibouin, F., Della Valle, G. & van der Sman, R., (2019b). Viscosity of artificial chewed boluses of  
429 cereal foods. *Edible Soft Matter 17th-19th April*, Le Mans, France.
- 430 Haward, S.J., Odell, J.A., Berry, M.A., Hall, T. (2011). Extensional rheology of human saliva. *Rheol*  
431 *Acta*, 50, 869–879
- 432 Kristiawan, M., Micard, V., Maladira, P., Alchamieh, C., Maignret, J-E., Réguerre, A-L., Emin, A., Della  
433 Valle, G. (2018). Multi-scale structural changes of starch and proteins during pea flour  
434 extrusion. *Food Research International*, 108, 203–215.

435  
436  
437 Lambrecht, M.A., Deleu, L.J., Rombouts, I., Delcour, J.A. (2018). Heat-induced network formation  
438 between proteins of different sources in model systems, wheat-based noodles and pound  
439 cakes. *Food Hydrocolloids*, 79, 352-370  
440 Le Bleis, F., Chaunier, L., Montigaud, P., Della Valle, G. (2016). Deconstruction mechanisms of bread  
441 enriched with fibres during mastication. *Food Res. Int.*, 80, 1-11.  
442 Loret, C., Walter, M., Pineau, N., Peyron, M. A., Hartmann, C., Martin, N. (2011). Physical and related  
443 sensory properties of a swallowable bolus. *Physiology & Behavior*, 104, 855-864  
444 Marconati, M., Engmann, J., Burbidge, A.S., Mathieu, V., Souchon, I., Ramaioli, M. (2019). A review of  
445 the approaches to predict the ease of swallowing and postswallow residues. *Trends in Food*  
446 *Science & Technology* 86, 281–297  
447 Morell, P., Hernando, I., Fiszman, S.M. (2014). Understanding the relevance of in-mouth food  
448 processing. A review of *in vitro* techniques. *Trends in Food Science & Technology* 35, 18-31  
449 Mosca, A.C. & Chen, J. (2017). Food-saliva interactions: Mechanisms and implications. *Trends in Food*  
450 *Science & Technology* 66, 125-134  
451 Núñez, M., Della Valle, G., Sandoval, A. J. (2010). Shear and elongational viscosities of a complex  
452 starchy formulation for extrusion cooking. *Food Res. Int.*, 43, 2093-2100.  
453 Pentikäinen S, Sozer N, Närväinen J, Ylätaalo S, Teppola P, Jurvelin J, Holopainen-Mantila U, Törrönen  
454 R, Aura AM, Poutanen K. (2014) Effects of wheat and rye bread structure on mastication  
455 process and bolus properties. *Food Res Int* 66:356–364  
456 Saboo, N., Kumar, P. (2018). Equivalent slope method for construction of master curves. *Indian*  
457 *Higways*, February, 19-28.  
458 van der Sman R.G.M., Mauer L.J. (2019). Starch gelatinization temperature in sugar and polyol  
459 solutions explained by hydrogen bond density. *Food Hydrocolloids*, 94, 371–380  
460 Stokes, J.R. , Boehm, M.W., and Baier, S.K. (2013). Oral processing, texture and mouthfeel: From  
461 rheology to tribology and beyond". *Current Opinion in Colloid & Interface Science* 18, 349-  
462 359.  
463  
464



465 **List of figures**

466 Figure 1: Examples of mechanical spectra obtained for the artificial bolus in the linear viscoelastic  
467 domain ( $\gamma < 0.5\%$ ) for (a) standard sponge cake (SC), (b) sponge cake enriched with plant  
468 proteins (SCP), (c) extruded flat bread (EF) and (d) extruded pea flour (EFP) for different  
469 levels of water content WC as indicated in the graphs, on a total wet basis (the darker the  
470 symbols, the larger the WC value).

471  
472 Figure 2: Variation of storage modulus  $G'$  at viscoelastic plateau ( $\omega = 1\text{rad/s}$ ) as function of the water  
473 content of food bolus for SC (O, a), SCP (●, b), EF (□, c) and EFP (■, d). Straight lines feature  
474 fitting by exponential functions ( $r^2 > 0.96$ ) with parameters given in Table 2.

475  
476 Figure 3: Example of strain sweep test result (here for SCS bolus, WC=0.57). Dotted vertical lines  
477 delineate the three regimes of bolus behavior, viscoelastic, plastic and flow. The crossing  
478 point ( $G' = G''$ ) allows defining the characteristic stress  $\tau_c$ .

479  
480 Figure 4: Variation of characteristic stress  $\tau_c$  at modulus crossing ( $G' = G''$ ) as function of the water  
481 content of food bolus for SC (O), SCP (●), EF (□) and EFP (■). Straight lines feature fitting by  
482 exponential functions ( $r^2 > 0.96$ ) with parameters given in Table 2.

483  
484 Figure 5: Flow curves of cereal food boluses obtained by capillary rheometry, for three different  
485 moisture contents WC (lowest O, medium ●, highest ●): SC (a), SCP (b), EF (c) and EFP (d).  
486 Dotted lines are best fit by power law functions ( $r^2 > 0.75$ ).

487  
488 Figure 6: (a) Variations of the shift factor  $a$  applied to build a master curve from curves represented  
489 in Fig.5, with water content WC for SC (O), SCP (●), EF (□) and EFP (■), dotted line showing  
490 best fit  $a = 8.10^{-4} \exp [12 \cdot WC]$  ( $r^2 \approx 0.89$ ); and (b) flow curves derived from the Herschel-  
491 Bulkley model applied for artificial bolus at WC=0.6, of sponge cake (black lines, SC and SCP)  
492 and extruded bread (grey lines, EF and EFP), standard cereal foods (thin continuous, SC and  
493 EF) and enriched in legume protein (dotted thick, SCP and EFP).

494  
495 Figure 7: Variations of Herschel-Bulkley model's coefficients (defined in eq. (4) and (5)) with water  
496 content of food bolus for SC (O), SCP (●), EF (□) and EFP (■): yield stress  $\tau_{sc}$  (a) and  
497 consistency  $K_c$  (b). Straight lines feature fitting by exponential functions ( $r^2 > 0.96$ ) with

498 parameters given in Table 2, whereas thick dotted line (light grey) in (b) features the best fit  
499 obtained by taking all boluses together into account ( $K_c = 180 \exp [-10.25 * WC]$ ,  $r^2=0.9$ ).

500

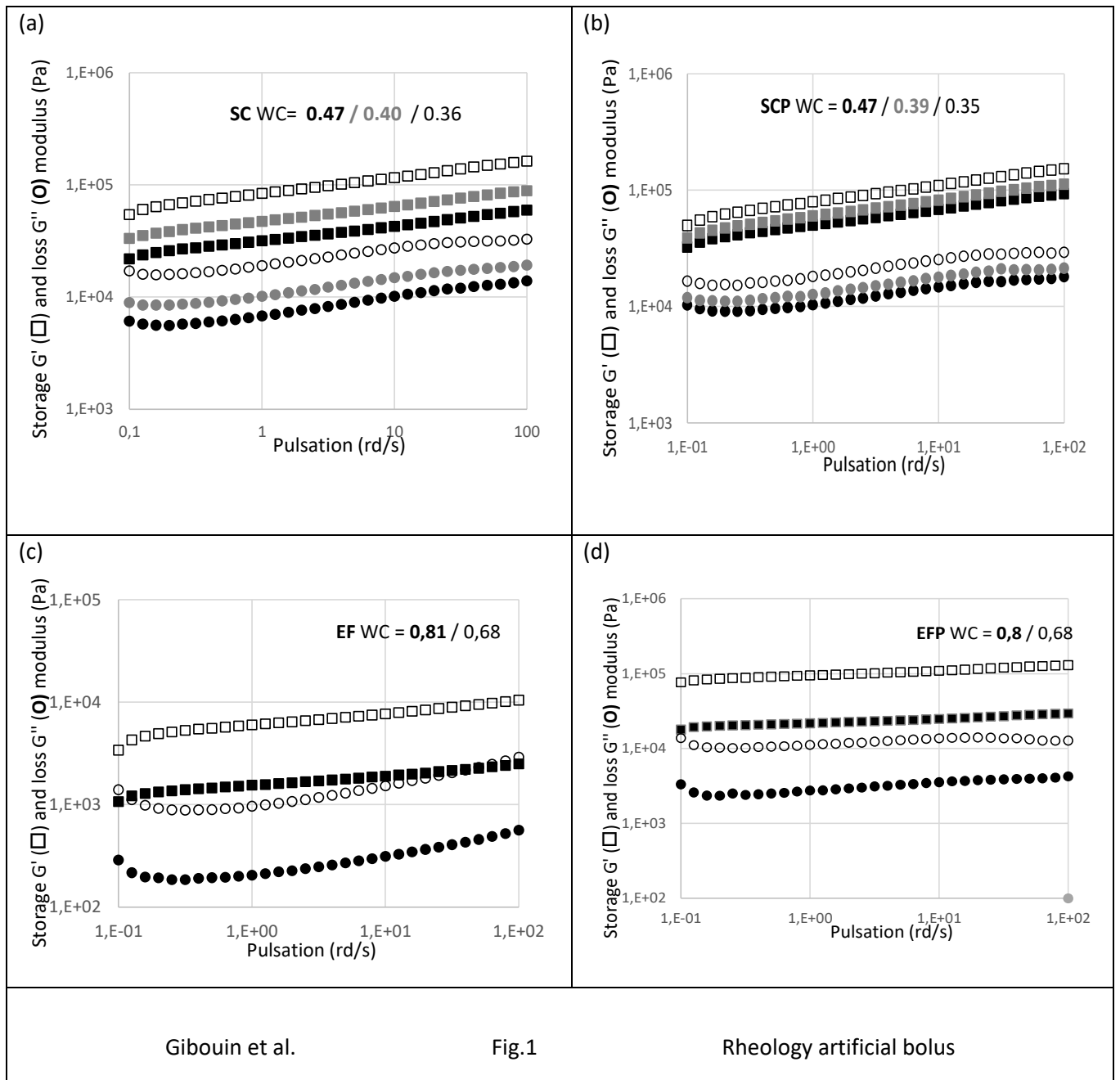
501 Figure 8: Micrographs of the artificial boluses of (a) standard sponge cake SC, (b) sponge cake  
502 enriched with proteins (SCP, white stain on bottom left is water between food particles), (c)  
503 extruded flat bread (EF) and (d) extruded pea flour EFP. Image width is 1cm. No specific  
504 staining was used, so differences of shade (light / dark) reflect the matter concentration, i.e.  
505 non-uniform thickness of the sample layer between blades, rather than specific composition  
506 or structural state.

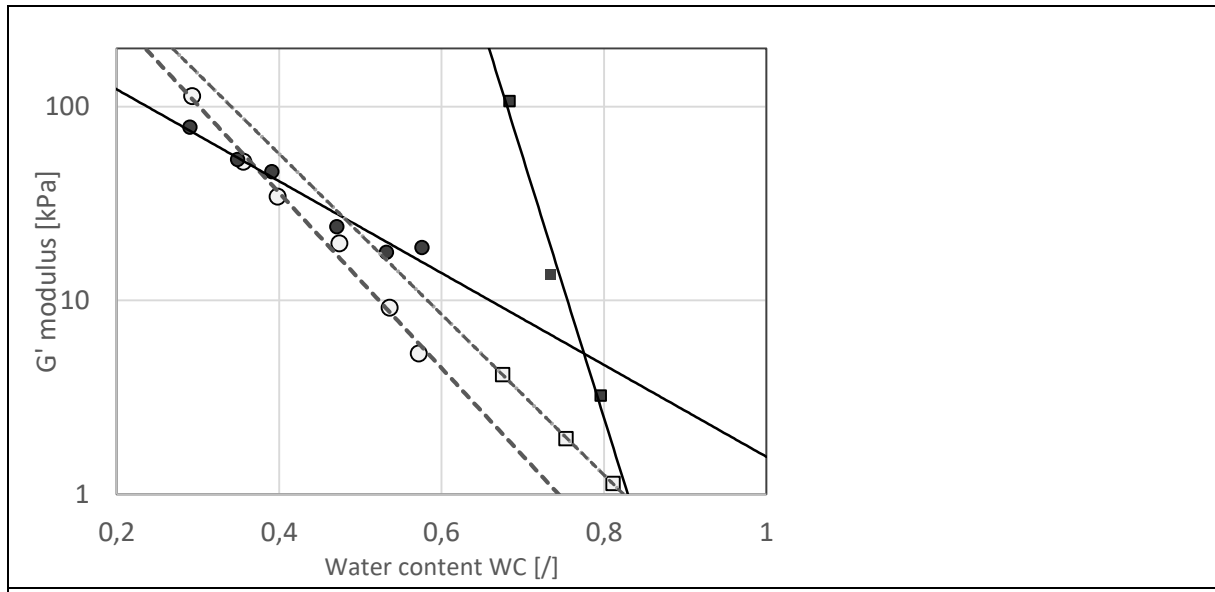
507

508 Figure 9: Schematic representation of bolus structure, envisioned as a suspension of more or less  
509 swollen and deformable spherical particles: dry ground food ( 1mm) (a), wet particles in low  
510 strain domain (or  $\tau < \tau_s$  or  $\tau_c$ ) (b); destructured suspension of particles of standard (c) and  
511 protein enrich foods (red spots symbolize proteic component (d)), at large strain ( $\tau > \tau_s$  or  $\tau_c$   
512 ).

513 Figure 10: Variations of the values of yield stress  $\tau_s$  computed for the same WC as characteristic  
514 stress  $\tau_c$  for the boluses of the four cereal foods SC (O), SCP (●), EF (□) and EFP (■).

515



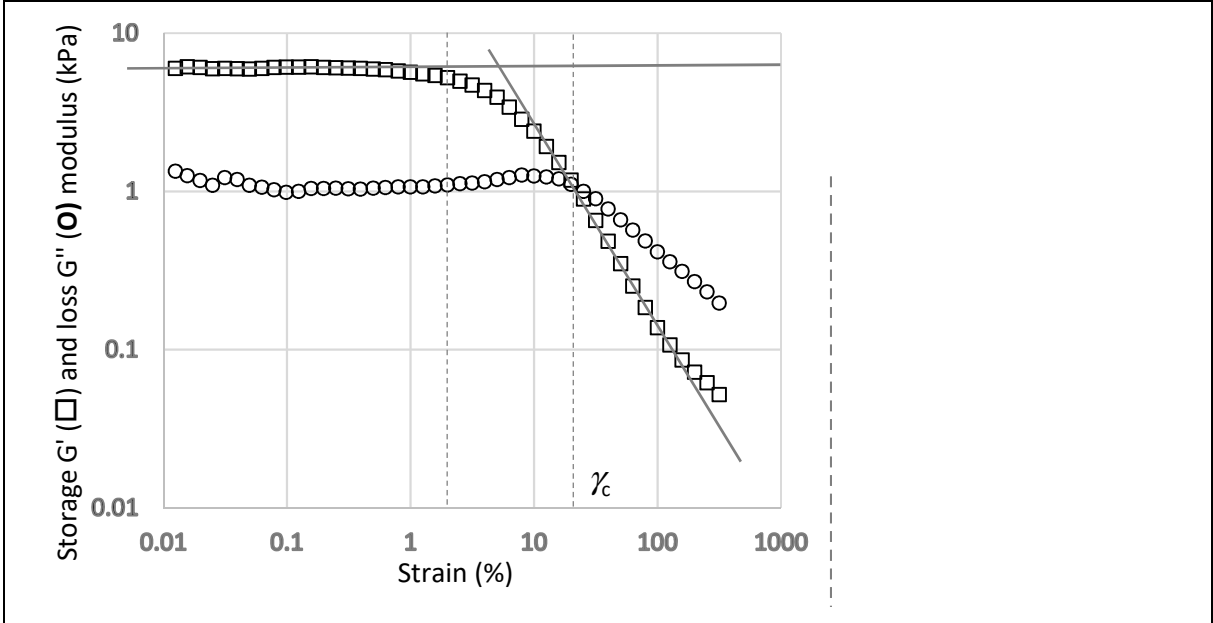


Gibouin et al.

Fig.2

Rheology artificial bolus

519



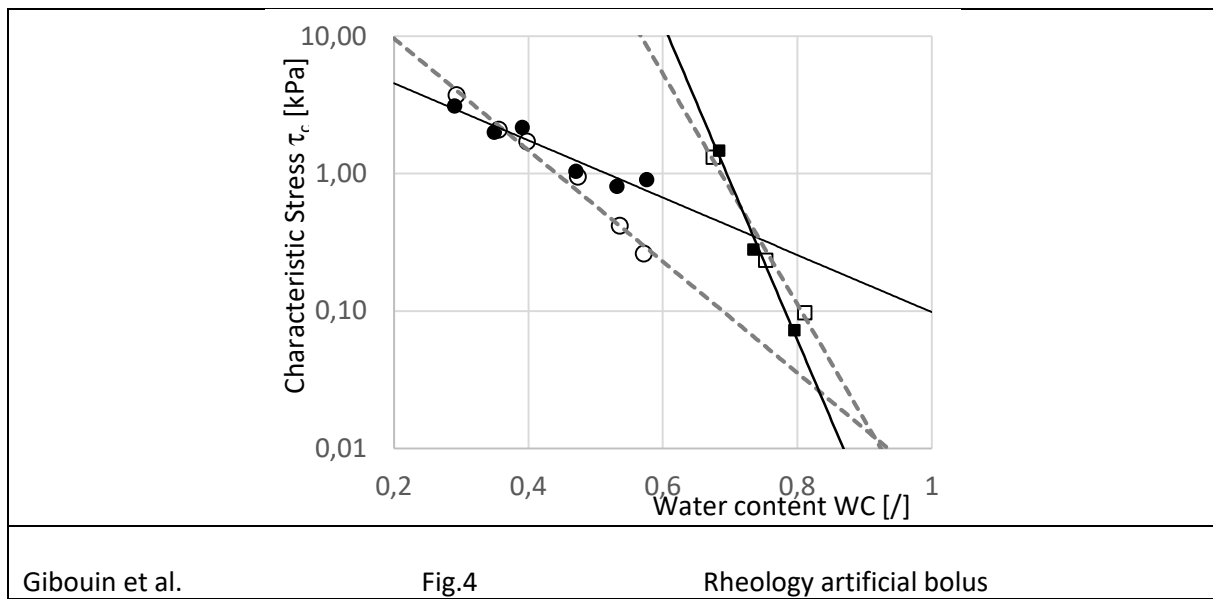
Gibouin et al.

Fig.3

Rheology artificial bolus

520

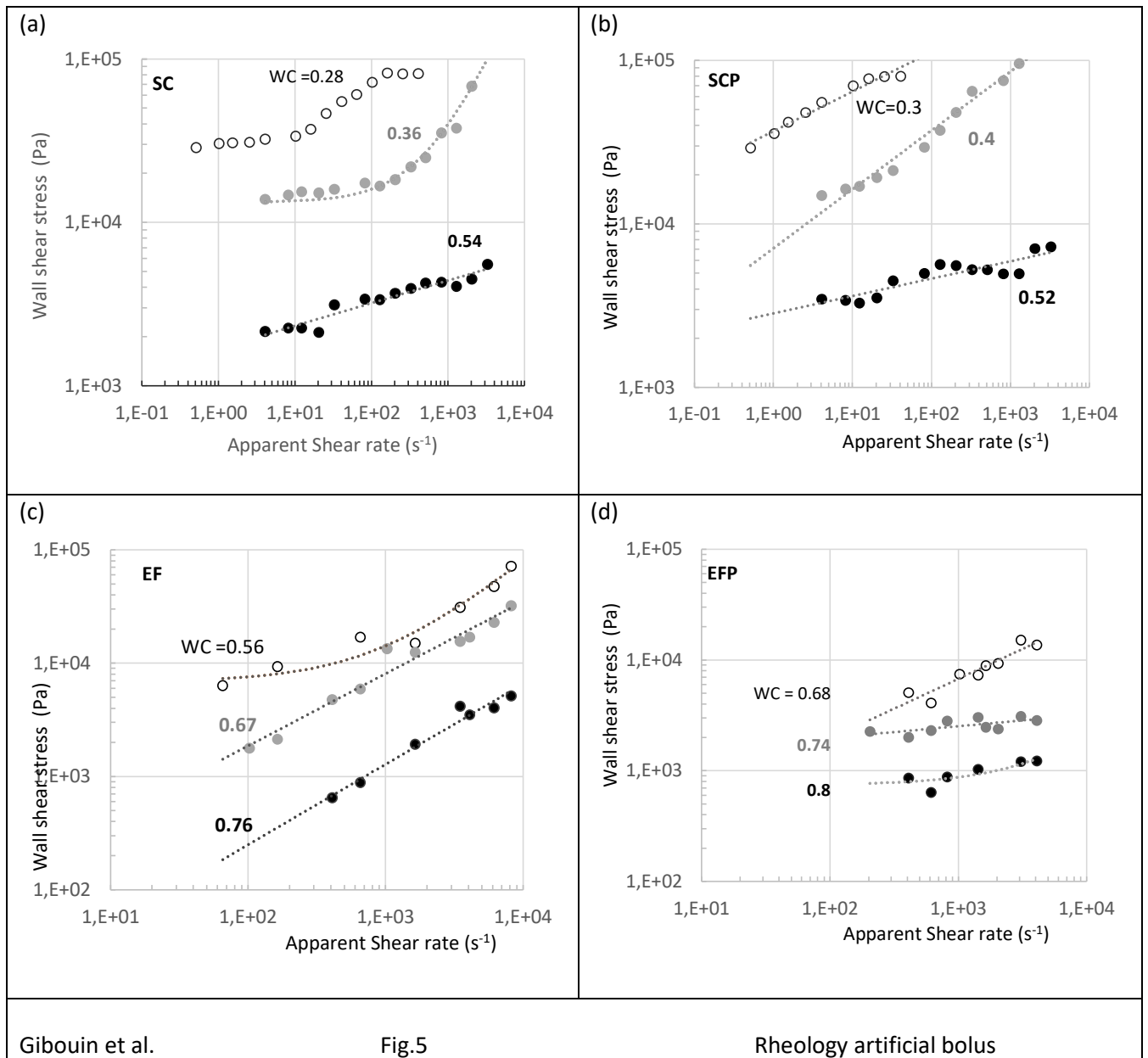
521



Gibouin et al.

Fig.4

Rheology artificial bolus



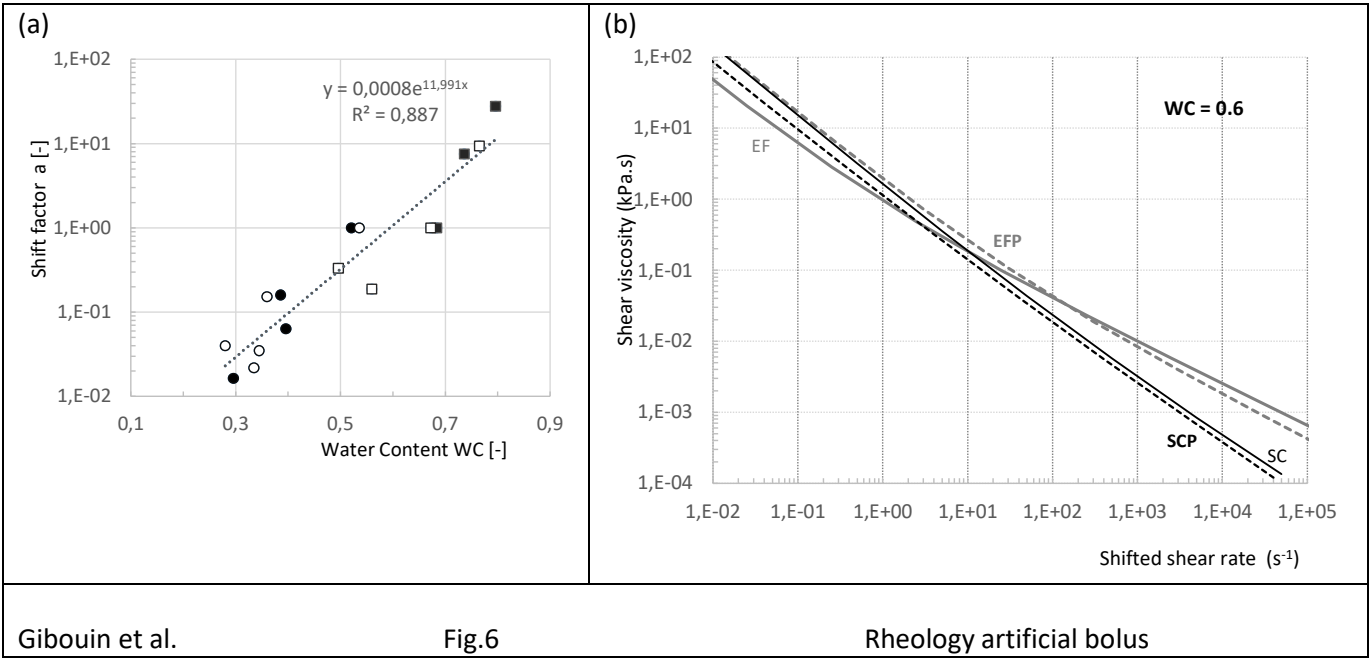
Gibouin et al.

Fig.5

Rheology artificial bolus

524

525



Gibouin et al.

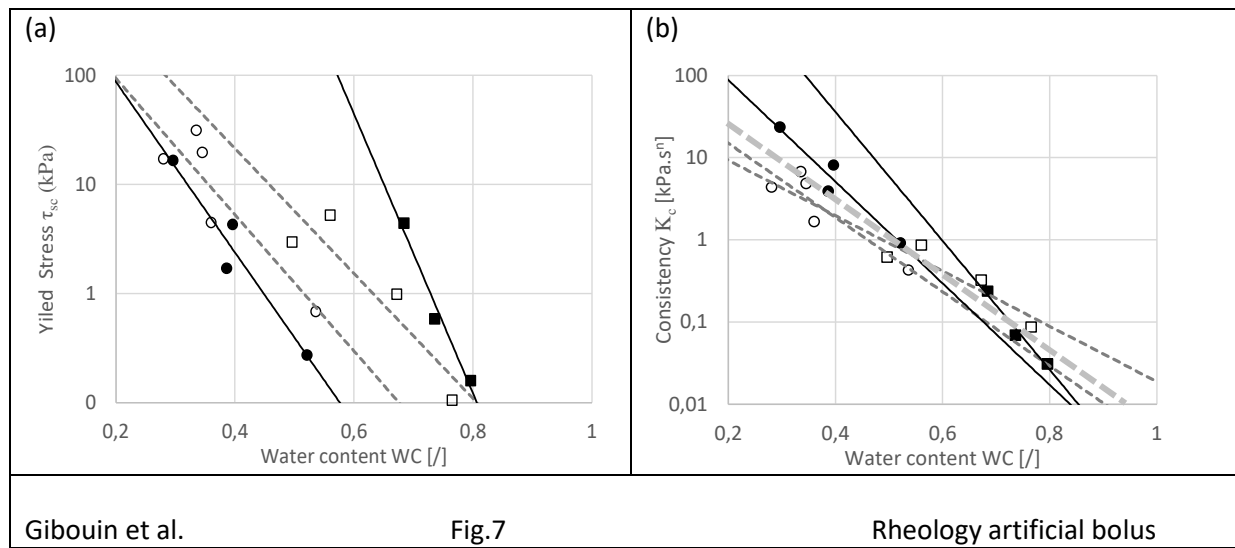
Fig.6

Rheology artificial bolus

526

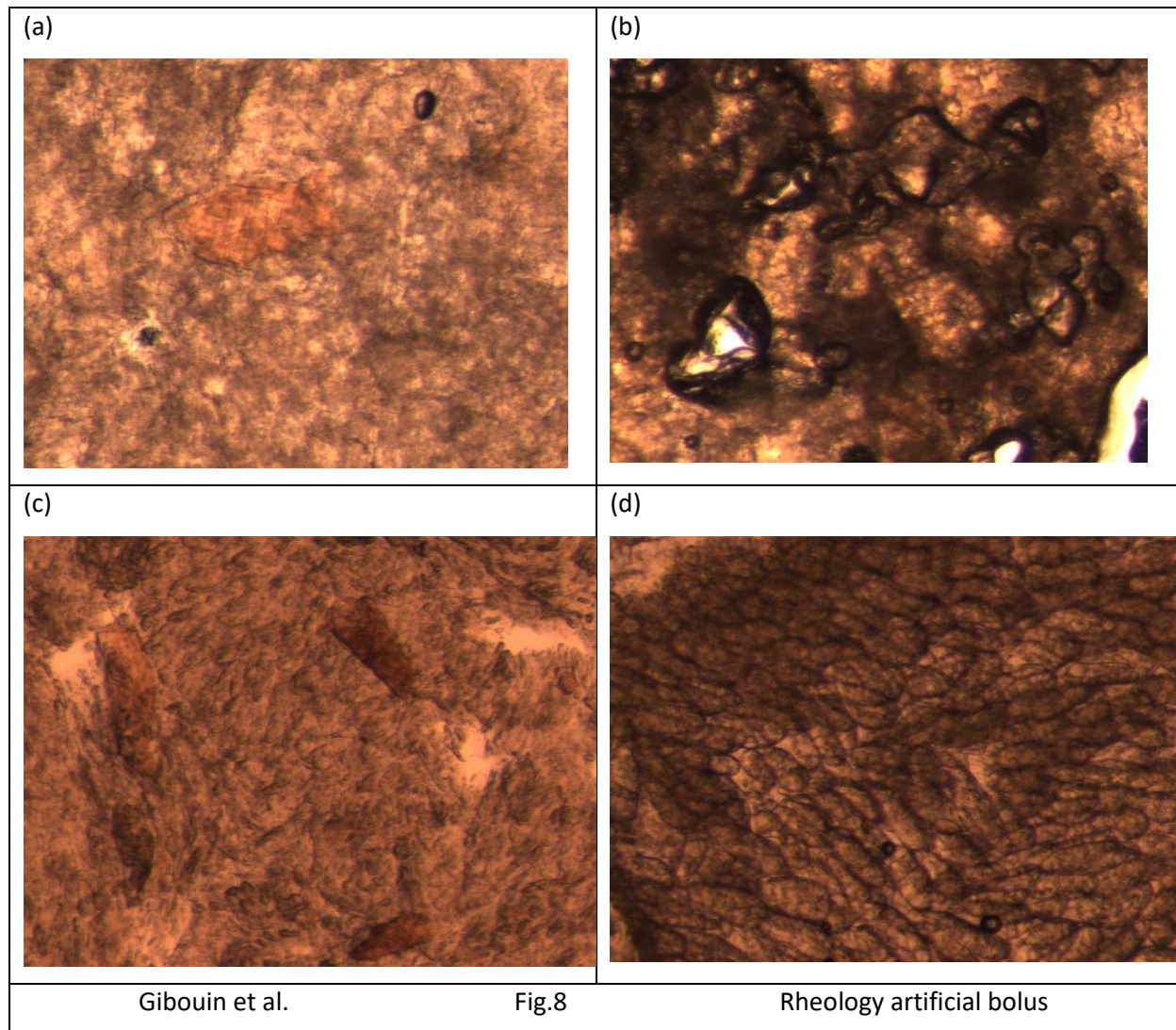
527





531

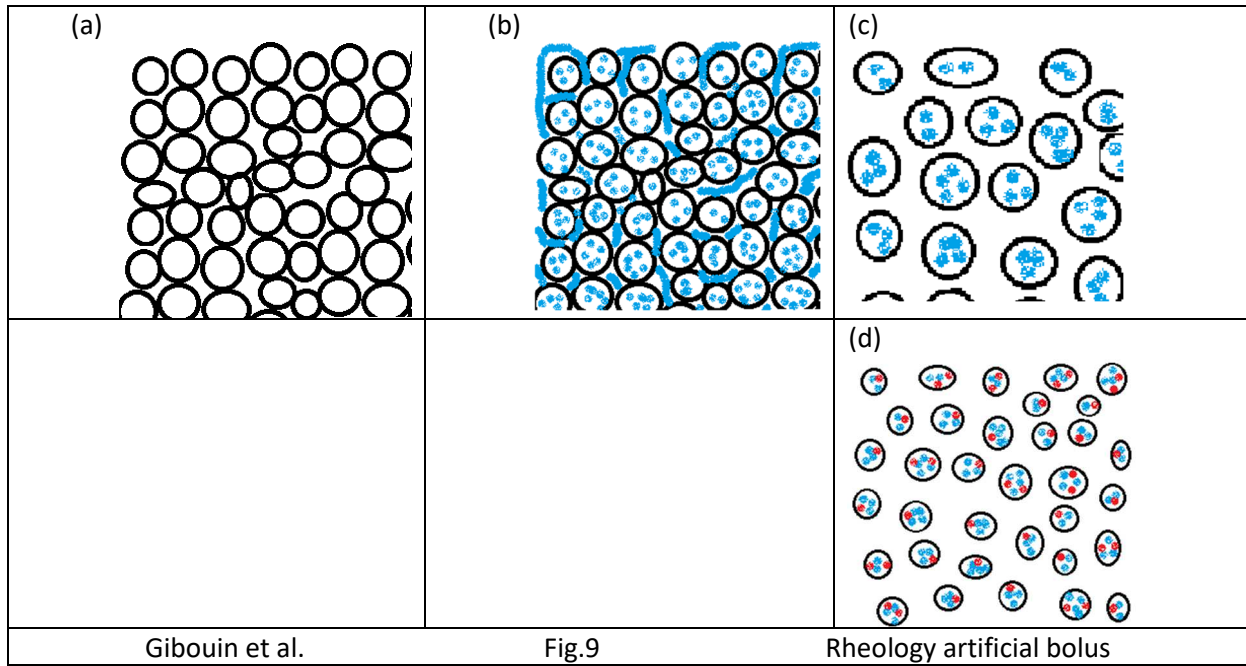
532



533

534

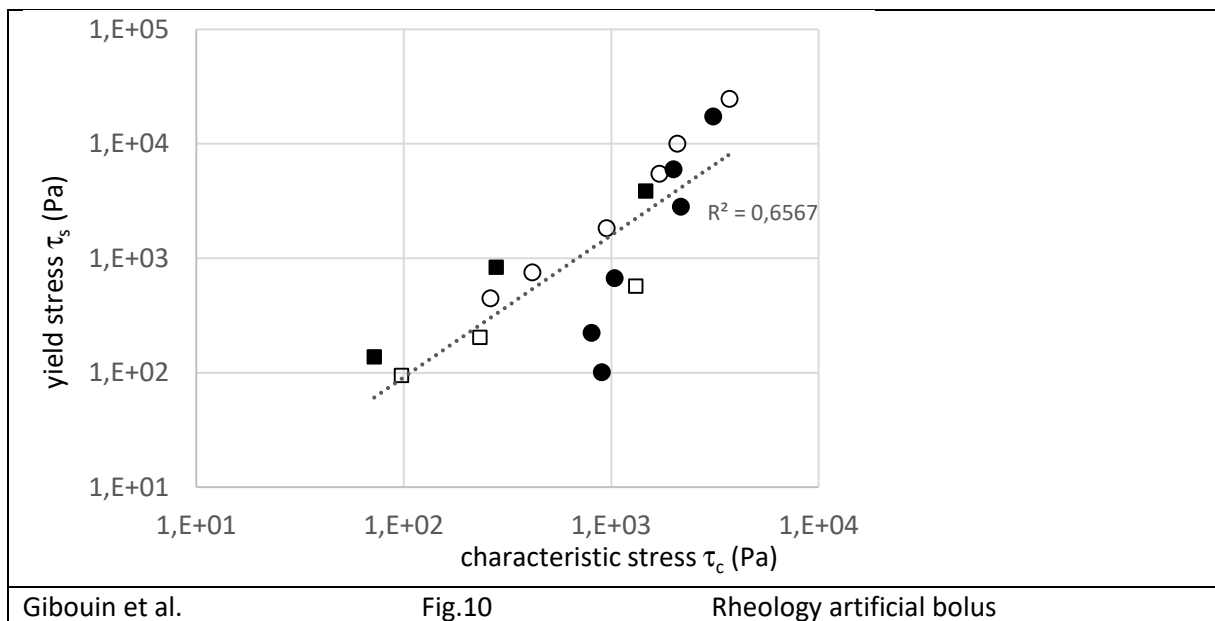
535



536

537

538



539

540

541

542 Table 1: Composition (% total wet basis) and density of the four tested foods, sponge cake (SC) and  
 543 extruded (E), and their protein enriched version (SCP and EFP).

Food Code name	Sponge cake		Extruded	
	SC	SCP	EF	EFP
Protein	11	13	13	23
Fat	6	5	5	-
Starch	18	13	67	42
Sugar	27	26	4	3
Cellulosic compounds (+ others)	10	13	5	22
Water content (% tot. wet mat.)	28	30	5	10
Density (g.cm <sup>-3</sup> )	0.21	0.23	0.14	0.15

544

545

546 Table 2: Values of the parameters of the models representing the relations between bolus  
 547 rheological properties and water content WC (see eqs 1, 3, 6).

Parameter	Viscoelastic domain				Flow regime			
	$G'_0$ MPa	$\alpha_G$	$\tau_{c0}$ kPa	$\alpha_{\tau_c}$	$\tau_{s0}$ kPa	$\alpha_{\tau}$	$K_{c0}$ kPa.s <sup>n</sup>	$\alpha_K$
Food								
SC	2.34	10.4	57.7	9.3	1670	14.4	120	10.4
SCP	0.37	5.5	12	4.8	3190	18.0	1510	14.2
EF	2.6	9.5	5.8 10 <sup>5</sup>	19.3	4200	13.2	44	7.7
EFP	1.4 10 <sup>8</sup>	30.8	1.04 10 <sup>8</sup>	26.5	2.15 10 <sup>9</sup>	29.5	49110	18

548

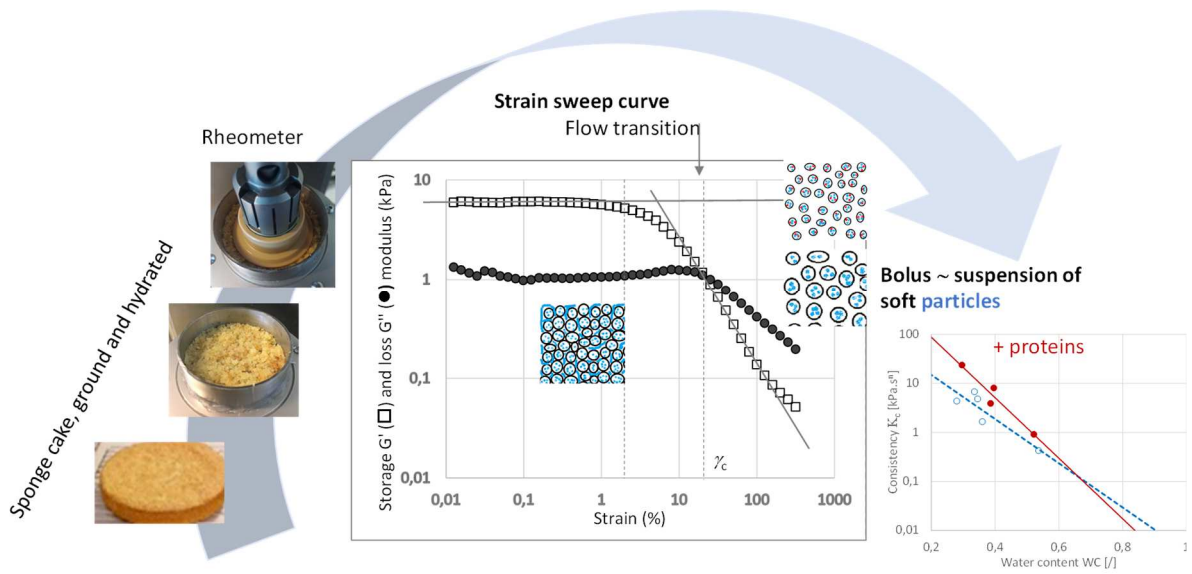
549

550 Table 3: Values of Herschel-Bulkley coefficients (see eq. (4)) for each product at chosen reference  
 551 value of WC.

Food	WC ref	$\tau_s$ (Pa)	$K$ (Pa.s <sup>n</sup> )	n
SC	0.54	685	430	0.28
SCP	0.52	270	915	0.21
EF	0.67	985	325	0.41
EFP	0.68	4410	235	0.39

552

553



Graphical abstract of measuring rheological properties of artificial boluses of cereal foods and determining interaction coefficient.